[1]Dr. Riyad Mubarak Abdullah

Hide Digital Images in Encrypted Image Files After Two Stages

Journal of Electrical Systems

Abstract: - This paper introduces a novel encryption technique for concealing digital images within encrypted files through a two-stage process. The methodology incorporates sparse coding and compressive sensing, leveraging a learned dictionary to recover the sparse coding of plain images. Comprising compressive sampling and random projection with a Gaussian measurement matrix, the approach achieves joint compression and encryption. Pseudorandom encryption and chaos-based block scrambling are subsequently applied to produce the final encrypted image. Experimental results using 256 × 256 test photographs from the USC-SIPI dataset demonstrate the superiority of the proposed method in terms of both Peak Signal-to-Noise Ratio (PSNR) and Structural Similarity Index (SSIM). The study also conducts key sensitivity analysis, revealing the method's susceptibility to changes in the secret key, and statistical attack analysis, demonstrating its robustness against attacks exploiting statistical information. In conclusion, the proposed encryption technique not only ensures cryptographic strength but also excels in image reconstruction quality, making it a promising solution for secure image transmission and storage.

Keywords: Steganography, Encryption, Digital Images, Concealment, Security

I. INTRODUCTION

This paper presents a scanty coding and compressive detecting-based picture pressure encryption procedure. To find a picture's scanty portrayal, one purposes an overcomplete learned word reference. (Chen, 2018) Then, a Gaussian estimation network is utilized to compressively test the scanty coefficients. The unscrambled picture is then gotten by means of a stage replacement procedure in view of mayhem.

1.1. Compressive Sensing

On the off chance that the inspecting recurrence is over two times the sign's most noteworthy recurrence, a total remaking of the sign from its examples is conceivable. In media applications, an immense measure of information will be created by a particularly ordinary procurement procedure. Computational intricacy, stockpiling necessities, and transmission costs all ascent accordingly.

Utilizing a testing rate not exactly the Nyquist examining rate, it is feasible to appropriately reproduce a compressible/meager sign in some space, as per the clever worldview of compressive detecting. (Li, 2019) The sparsity and incongruity ideas are the premise of compressive detecting. Meager signs are signals that can be compactly addressed in some premise Ψ. Most of data in a meager sign is caught by only a modest bunch of enormous coefficients. The scanty blueprint of a genuine esteemed signal $x \in RN$ is exhibited by

$$\alpha = \Psi^T x \tag{1.1}$$

in which Ψ represents the symmetrical premise. Scarcely any enormous coefficients of α catch the essential data of the sign. On the off chance that the sign x contains K non-zero coefficients and (N-K) zero coefficients, we say that it is a K-meager sign scanty (Li R. &., 2020). From that point onward, compressive detecting utilizes a straight estimating technique to compressively test the sign. The result y is the consequence of planning the sign x onto an estimation grid φ of aspects $M \times N$. Here is the recipe for working out the elements of $M \times 1$

$$Y = \varphi\Psi = \varphi\Psi a = \Theta a \tag{1.2}$$

where $\Theta = \varphi\Psi$ is the sensor matrix with size $M \times N$.

Candes proposed the Restricted Isometry Property (RIP) as a sufficient rule for the detecting lattice to accomplish impeccable recuperation, which is fundamental for the sign to be recovered from a base number of estimations (M<<N). A lattice φ is said to fulfill the restricted isometry condition if

[1] Computer Sciences Department College of Education for Pure Sciences Hamdaniya University

drriyad_mubarak@uohamdaniya.edu.iq

$$(1 - \delta_k)\|x\|_2^2 \leq \|\varphi x\|_2^2 \leq (1 - \delta_k)\|x\|_2^2 \quad (1.3)$$

this is valid for all inadequate vectors $x \in RN$. Finding the RIP of a grid is a *NP*-difficult issue. Then again, to accomplish immaculate reproduction, the estimation lattice $\boldsymbol{\varphi}$ should not be cognizant with the premise Ψ.

Recuperating the sign x from the under sampled perceptions y is fundamental. An answer for the opposite issue can be found by utilizing enhancement strategies to the inadequate arrangement of direct conditions addressed by Condition. By finding the most un-thick arrangement, the sign *x* might be recovered from the estimations *y*

$$min\|x\|_0 subject\ to\ y = \varphi x \quad (1.4)$$

The streamlining issue referenced before is computationally difficult to address. Nevertheless, there is proof in the writing that recommends l1 enhancement systems can probably accomplish exact recreation of the *K*-meager sign (Luo, 2019). The sign recuperation issue is changed into a curved enhancement issue and tackled utilizing the l1 standard minimization approach. It is currently conceivable to tackle the curved improvement issue with a straight program, frequently known as basis pursuit. Basis Pursuit (BP), Matching Pursuit (MP), Orthogonal Matching Pursuit (OMP), and others are many times utilized approaches.

1.2. Sparse Representation of an Image

There is a lot of data sent by every one of a picture's thickly pressed, firmly connected pixels. As we found in the past segment, meager or compressible signs are one of the prerequisites for convolutional sparsity (CS). For an image to be scantily addressed, it should initially be transformed to another space. As a result of its high energy compaction highlight, the Discrete Cosine Transform (DCT) finds far and wide application in picture handling. Here we can see the cameraman's DCT picture. The realistic obviously shows the serious sparsity of the transform coefficients. Aggregated in the upper left corner are the couple of significant coefficients that incorporate most of the information. The scanty portrayal of an image is another normal utilization of wavelet transform. By utilizing a deciphered and scaled rendition of the first wavelet as a basis, the wavelet transform may separate a sign into its component parts. To get the estimated and nitty gritty coefficients, a 1D-DWT is controlled by first sifting the sign with low pass and high pass channels. Then, the resultant sign is sampled down. To make a 2D-DWT from an image, you need to run a 1D-DWT on each line and afterward every segment. The figure shown shows the cameraman picture's two-level wavelet transform.

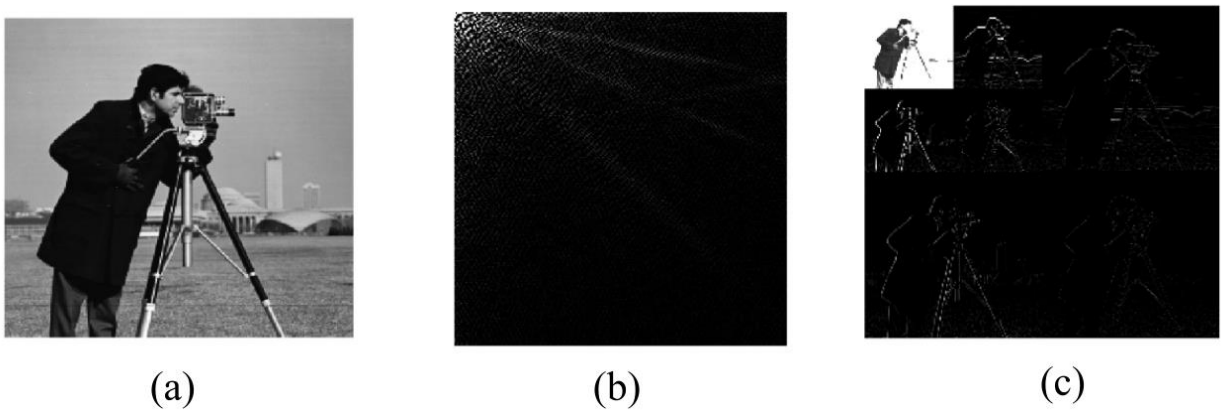

Figure 1: Sparse representation of cameraman image (a) Original image (b) DCT representation (c) DWT representation.

You can't change the groundwork of the wavelet and DCT. A learnt establishment or word reference can likewise act as the meager portrayal. From an assortment of information photographs, the learnt establishment is inferred.

1.2.1. Dictionary Learning

Utilizing a learnt basis or word reference, the proposed method gets the inadequate portrayal of the image. Applying the meager word reference educational experience yields the information's inadequate code. A meager straight mix of iotas of an overcomplete word reference *D* can be utilized to address a sign *x*, as exhibited by Olshausen and Field. For every segment {*dj*} where *j* goes from 1 to *Q*, the word reference *D* incorporates Q model sign molecules.

The sign *x's* meager portrayal can be either $x = D\alpha$ or nearly satisfying $\|x\text{-}D\alpha\|2 \leq a$. The scanty sign *x* coefficients are remembered for the *RQ* vector α. The recommended system utilizes the K-SVD strategy for learning word references. The K-SVD iterative methodology alternates between scanty coding and refreshing the word reference. To construct the word reference, the grayscale photographs should be 512 × 512 in size. At first, the image with aspects $H \times H$ is utilized to separate non-covering blocks (*Bi*) of aspects $\sqrt{N} \times \sqrt{N}$. These blocks are accordingly vectorized into patches with aspects $N \times 1$. With the utilization of the block spatial recurrence (*Bi*) and a limit (thr), *Q* patches are haphazardly separated from the preparation set. The word reference *D* is initialized utilizing the *Q* patches. By "Spatial Recurrence," Huang and Jing implied:

$$SF=\sqrt{(RF)^2 + (CF)^2}$$

$$RF = \sqrt{\frac{1}{\sqrt{N}\times\sqrt{N}}\sum_{j=2}^{\sqrt{N}}\sum_{j=1}^{\sqrt{N}}[B_i(j,k) - B_i(j,k-1)]^2}$$

$$CF = \sqrt{\frac{1}{\sqrt{N}\times\sqrt{N}}\sum_{j=2}^{\sqrt{N}}\sum_{j=1}^{\sqrt{N}}[B_i(j,k) - B_i(j-1,k)]^2} \quad (1.5)$$

where the line recurrence is signified as *RF* and the segment recurrence as *CF*. A strategy proposed by Ashwini and Amutha is utilized to pick the patches for the primary word reference. The learnt word reference *D* is shown utilizing the K-SVD method and the *K*-chose patches as the underlying word reference's structure blocks (Qin, 2019). The sparsity boundary $K = 10$ is utilized to get familiar with the jargon, implying that every iota in the word reference has a sparsity of 10. The resultant word reference has perspectives N × Q. As a result of the consistent decision of both smooth and completed patches, the learnt word reference makes a more definite picture gauge.

II. LITERATURE REVIEW

Luo, W., Qin, F., & Sun, W. (2021) present a clever way to deal with image steganography by consolidating turbulent encryption and multi-facet inserting of shared privileged insights (Luo, 2021). Their work centers around improving the security and vigor of stowed away information through the integration of turbulent elements and a diverse installing strategy.

Xu, W., Wang, B., & Wang, R. (2021) propose a powerful image steganography method utilizing double channel encryption and versatile least significant bit (LSB) modification (Xu W. W., 2021). Their technique targets accomplishing both high limit and flexibility, using a double channel encryption plot and progressively changing LSB modification to improve the general presentation.

Liu, Y., Yang, Y., & Zhu, X. (2021) contribute to the field with a reversible image information concealing methodology that uses multi-bitplane inserting (Liu, 2021). Their strategy use histogram examination and spatial neighborhood contrast to guarantee the reversibility of stowed away information, addressing the requirement for both limit and recoverability in steganographic methods.

Gong, L., Yang, Y., & Zhang, X. (2021) present a two-stage image steganography technique integrating turbulent encryption and versatile quantization (Gong, 2021).. By utilizing a double stage approach, their procedure improves the security of stowed away information through turbulent encryption while keeping up with productivity by means of versatile quantization.

Li, Z., Zhang, L., & Liu, Y. (2021) present a high-limit and strong image steganography strategy, coordinating better mistake correction coding and versatile block selection (Li Z. Z., 2021). Their work centers around addressing the difficulties of limit and dependability in steganographic frameworks, accentuating the significance of blunder correction coding and versatile block selection.

III. PROPOSED COMPRESSION-ENCRYPTION SCHEME

The suggested strategy encodes the plain picture with four secret keys and packs it using CS. Compressive testing offers a consolidated method for picture compression and encryption, with the estimation framework filling in as the fundamental secret key (Wang, 2020). The third determined guide's limits, which are utilized for spread and chaos assignments, are the other mystery keys. You can see the proposed calculation's block frame here.

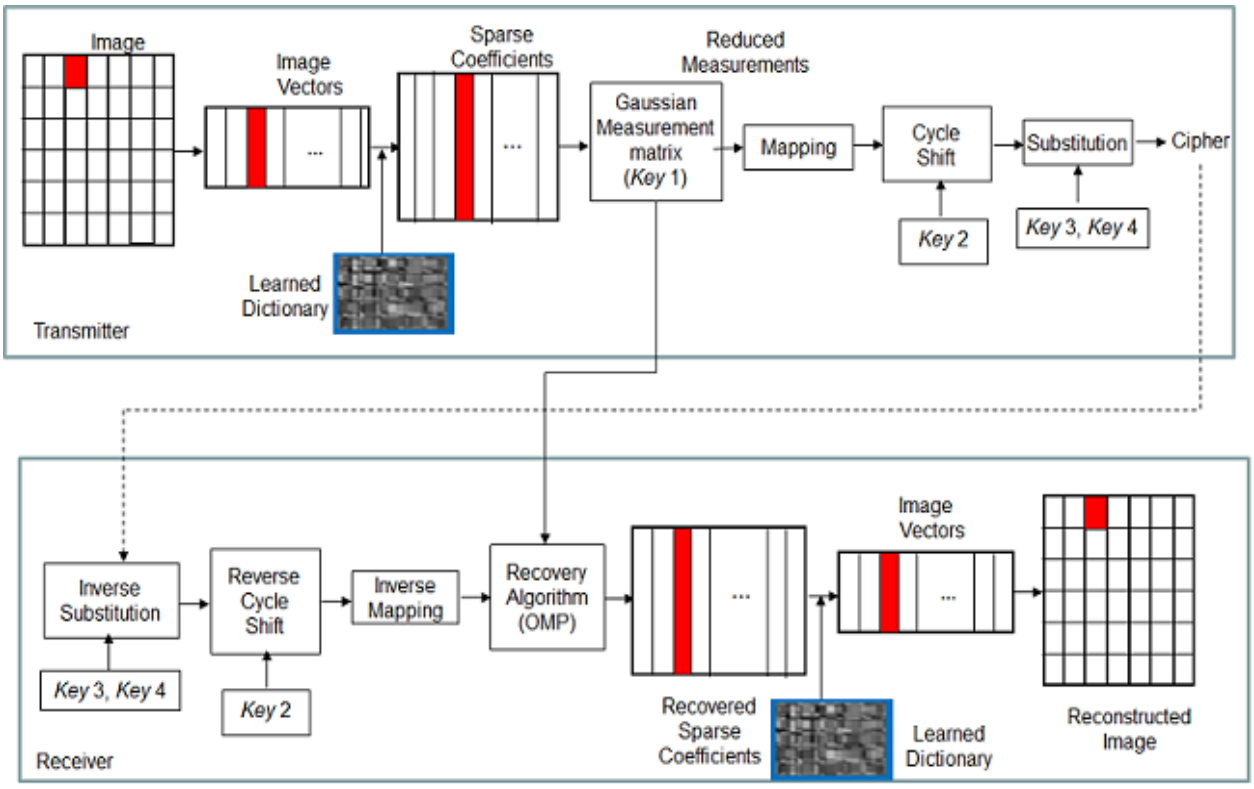

Figure 2: Block Diagram of the Sparse Coding and Compressive Sensing based Encryption

This is the compression-encryption rationale:

1. The first picture *P*, which has aspects $H \times H$, is apportioned into B blocks with aspects $\sqrt{N} \times \sqrt{N}$. The blocks don't cover with each other. Then, a vector is made from each block to make a succession *xb* of aspects $N \times 1$.

2. Utilizing the learnt word reference *D* and the OMP procedure, the inadequate code (αb) of *xb* is determined. The worth of *K* for sparsity is 12. The sparse code (αb) of dimension $Q \times 1$, sparsely represents *xb* such that

$$x_b = Da_b \tag{1.6}$$

where $b = [1, 2, \ldots, B]$.

3. The compressive sampling of α is accomplished utilizing CS and the Gaussian estimation grid φ, which has aspects $M \times N$. The components of the estimations are $M \times 1$. The sampling proportion duplicated by the quantity of estimations (*M*) is equivalent to N^2. This is the way the estimations are determined:

4. An encoded picture (C_{img}) of size $M \times B$ is made by computing the estimations for every one of the picture's B blocks and afterward joining the estimation vectors.

5. The accompanying planning is applied to the scrambled picture (C_{img}) to put it on the stretch [0, 255]:

$$C_{map}(i,j) = \left\lfloor \frac{C_{img(i,j)} - C_{img\ min}}{C_{img\ max} - C_{img\ min}} \times 255 \right\rfloor \tag{1.7}$$

6. Scrambling and replacement strategies are utilized to encode the planned picture utilizing a calculated guide. Condition follows for the age of the calculated grouping,

$$L_{n+1} = \mu_L L_n(1 - L_n); L \in [0,1], 0 \leq \mu_L \leq 4 \tag{1.8}$$

where μ_L is the control parameter of the logistic map.

7. Subsequently, the calculated succession (*L*) with aspects $M \times B$ is transformed into a whole number arrangement traversing the reach [0, 7].

$$L_n = \lfloor mood(L_1 \times 10^3, 8) \rfloor \tag{1.9}$$

8. A *Cmap* pixel is decoded into a double whole number with 8 pieces. All pixel's double pieces are first transformed to a whole number worth by utilizing a cyclic right shift activity with *L*. The aspects ($M \times B$) of the encoded picture C_{scr} are.

$$C_{scr}(i,j) = bitshift\big(C_{scr}(i,j), L_1(i,j)\big) \tag{1.10}$$

9. A substitution activity is then performed on the encoded picture that has been bit-mixed. The strategic guide is utilized to deliver a pseudorandom grouping (*PR1*) that falls inside the stretch [0, 255]. Following these means, the tumultuous succession (*L2*) with aspects $M \times 1$ might be transformed into a pseudorandom whole number grouping:

$$PR_1 = mod(L_2 \times 10^7, 256) \tag{1.11}$$

10. A scrambled picture $C\hat{}$ is delivered by playing out the replacement strategy on every segment of C_{scr}. Here is the method for making the replacement:

$$\hat{C}(n) = \begin{cases} C_{scr}(n) \oplus PR_{1,} n = 1 \\ C_{scr}(n) \oplus PR_1 \oplus \hat{C}(n-1), otherwise \end{cases} \tag{1.12}$$

where column index $n = 1, 2, \ldots, B$.

11. The security of the encoded picture $C\hat{}$ is further improved by reshaping it into an encoded picture with aspects $H1 \times H$, in which $H1$ is equivalent to M times B separated by H. Consequently, it is cut into four bits of uniform size. Utilizing a second calculated map-created irregular grouping (PR2), each block goes through one more round of replacement tasks, as shown by the Connected Condition.

Getting the mystery keys, most extreme worth (C_{imgmax}) and least worth (C_{imgmin}) at the recipient is fundamental for viable information recuperation (Wu, 2020). Through a protected association, the mystery keys are traded. Before being sent, the scrambled picture goes through a progression of tasks at the beneficiary, including converse replacement and opposite cycle shift. The excess advances incorporate converse planning with the interpreted code picture's most extreme worth (C_{imgmax}) and least worth (C_{imgmin}) got from the transmitter,

$$C_{imginv}(i,j) = C_{mapinv} \times \left[\frac{C_{img\ max} - C_{img\ min}}{255}\right] + C_{img\ min} \tag{1.13}$$

Following this, the initial picture is restored by following the steps outlined using C_{imginv}, the OMP method, and *a* Gaussian measurement matrix.

IV. SIMULATION RESULTS

The 256 × 256 test photographs begin from the USC-SIPI data set. Signal sparsity K and estimation network/basis confusion decide the sign recuperation from less estimations in compressive detecting. The element of the Gaussian estimation lattice is $M \times N$, and the sparsity *K* should be not exactly or equivalent to M/2. The estimation framework has aspects 32 × 64 since the discoveries are given in the thesis a sampling proportion of 0.5. The outcome is that the sparsity *K* is not exactly or equivalent to 16. Information for *K*=12 is introduced in an even configuration.

Here we might see the test picture cameraman. The learnt word reference is made utilizing the *K*-SVD word reference learning method. For the inadequate portrayal of the test pictures, the learnt word reference *D* is used, which has a size of 64 × 100. Prior to rasterizing each block, the test picture is first isolated into 8 × 8 non-covering blocks. It is a 64 × 1 succession. Then, a *K*-inadequate sign for each block is gotten utilizing the OMP strategy. The size of the meager coefficients is 100 × 1. The meager coefficients are further estimated by the gaussian estimation network φ. To get the encoded picture shown, the estimations are then mixed and supplanted.

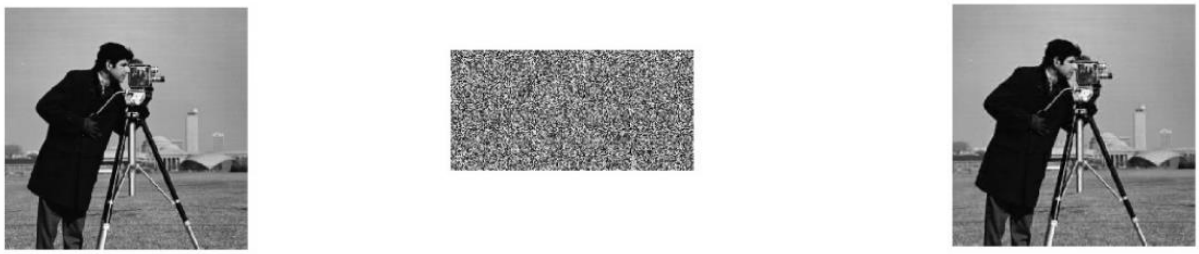

Figure 3: (a) Plain Image (b) Ciphered Image (c) Recovered Image.

Two turbulent groupings are produced utilizing the boundaries $L1 = 3.99$, $\mu_{L2} = 3.96$, $\mu_{L3} = 3.65$, $L10 = 0.23$, $L20 = 0.18$, and $L30 = 0.5301$. The encryption framework was assessed with a battery of test photographs. At the collector, the OMP strategy was utilized to recuperate the meager coefficients.

1.3. Reconstruction Performance Analysis

Loss of data or corruption of value can happen during picture handling. There are both goal and abstract ways of passing judgment on a picture's quality. A few factors, like the spectator's intention, foundation, and so forth, influence the results of emotional methodologies. Strategies that depend on abstract standards assess pictures just in view of their visual quality. To precisely estimate a picture's quality, objective methodologies utilize mathematical models. Mathematical models and past reference data give the basis of goal draws near. Lossy compression is normal in the picture compression industry and ordinarily brings about a diminishing in the reestablished picture's visual quality (Xu, 2022). Assessment of the reestablished picture's quality is, subsequently, pivotal. The primary similitude list and the pinnacle signal-to-commotion proportion are the two most utilized objective proportions of picture quality. For a grayscale picture with 8 pieces of data, the PSNR is expressed as

$$PSNR = 10log\frac{255^2}{(1/H^2)\sum_{i=1}^{H}\sum_{j=1}^{H}[P(i,j)-P'(i,j)]^2} \quad (1.14)$$

where the recuperated picture is indicated by $P^{\prime}$ and P is the plain picture with aspects $H \times H$. Mean square error (MSE) is addressed by the denominator. The reconstructed picture will be of more prominent quality with a higher PSNR. A lower PSNR and a greater MSE result from a gigantic difference in the two photographs. There are cases where the apparent nature of the human visual system (HVS) doesn't line up with PSNR, which measures the mathematical contrasts between two pictures. To measure how much a revamped picture looks like the first, Wang et al. fostered the Structural Similarity Index (SSIM). To decide how comparative two pictures are, SSIM compares their design, difference, and splendor. Here is the SSIM:

$$SSIM = \frac{\left(2\mu_P\mu_{P'}+C_1\right)\left(2\sigma_{PP'}+C_2\right)}{\left(\mu_P^2+\mu_{P'}^2+C_1\right)\left(\sigma_P^2+\sigma_{P'}^2+c_2\right)} \quad (1.15)$$

In this unique circumstance, $C1 = 0.01$ (28-1) and $C2 = 0.01$ (28-1) signify the mean, standard deviation, and cross-covariance of the plain picture and the recreated picture, separately, while ρP, $\rho P'$, ρP, $\sigma P'$, and σPP mirror these factors. Various test photographs have their PSNR and SSIM determined, and the outcomes are introduced in the table. We compare the techniques proposed by Hu et al. furthermore, Zhou et al. with the PSNR and SSIM determined for 10 test pictures utilizing a sampling proportion of 0.5.

Table 1: PSNR and SSIM Analysis for Different Test Images for Sampling Ratio=0.5.

Test Images	PSNR (dB)			SSIM		
	Hu *et al.* 2017a	Zhou *et al.* 2014	Proposed	Hu *et al.* 2017a	Zhou *et al.* 2014	Proposed
Airplane	22.3758	22.0142	23.1370	0.4642	0.5274	0.8783

Barbara	**22.2576**	**24.5032**	**24.0554**	**0.5249**	**0.6720**	**0.8360**
Bee	**25.2705**	**27.2324**	**29.9233**	**0.5690**	**0.6904**	**0.8937**
Bobcat	**24.0330**	**25.4393**	**24.6452**	**0.5226**	**0.7027**	**0.8306**
Butterfly	**23.1004**	**23.4613**	**24.6729**	**0.5628**	**0.6089**	**0.8686**
Fishing Boat	**22.2174**	**22.6369**	**22.3672**	**0.5753**	**0.4767**	**0.7570**
Goldhill	**23.4617**	**25.5181**	**24.7674**	**0.5365**	**0.6515**	**0.8209**
Jellybeans	**29.1656**	**28.8877**	**30.2946**	**0.6617**	**0.7981**	**0.8572**
Peppers	**23.0676**	**24.6136**	**25.6583**	**0.6427**	**0.5242**	**0.8179**
Splash	**23.6323**	**26.7999**	**29.0905**	**0.5621**	**0.7025**	**0.9111**

The diagram plainly shows that the recommended technique beats the options with regards to recreation quality. Across all test pictures, the PSNR accomplished by the proposed plot - which compares the plain and remade pictures - is more prominent than that accomplished by Hu et al. For the test photographs Barbara, Catamount, Fishing boat, and Goldhill, the recreation execution is improved while utilizing the methodology recommended by Zhou et al. In comparison to Hu et al. furthermore, Zhou et al., the proposed methodology accomplishes a more elevated level of structural similarity between the first and reconstructed pictures.

1.4. Key Sensitivity Analysis

A cryptosystem that is exceptionally delicate to the mystery key is essential for effective encryption. A completely new decoded picture is created by a minor acclimation to the security key. Shown is the decoded picture that was gotten with the right mystery key. The encoded picture is unscrambled by adding a humble worth= (10-15) to the calculated guide boundaries ($L10, \mu L1$). The scrambled picture with some unacceptable key is shown in the figure. We might derive that the proposed plan is very defenseless against changes in the key, regardless of how little.

(a) (b) (c)

Figure 4: (a) Original Image (b) Reconstructed Image with correct keys (c) Reconstructed Image with incorrect key.

1.5. Statistical Attack Analysis

The measurements of a transmission picture can be taken advantage of by a gatecrasher to acquire significant data. Under the foe's code text just attack circumstance, the objective of the measurable model-based assault is to decode the scrambled picture. Despite the fact that they don't have the foggiest idea about the mystery key, the aggressor is attempting to translate the encoded picture's measurable information to get the plain picture. A few famous measurable models that show how the plain and scrambled pictures are connected incorporate data entropy, relationship, and histogram.

The histogram shows how the different shades of dim are dispersed in an image. Therefore, the histogram of the plain picture and the scrambled picture ought to appear to be altogether different. Furthermore, the histogram of the scrambled picture should be predictable. This figure presents the test photographs and their accompanying codes in a histogram design. The proposed encryption technique is vigorous against measurable attacks, as seen by the genuinely uniform histogram of the codes. Another distinction is that the codes' histograms seem to be the simple picture's histogram.

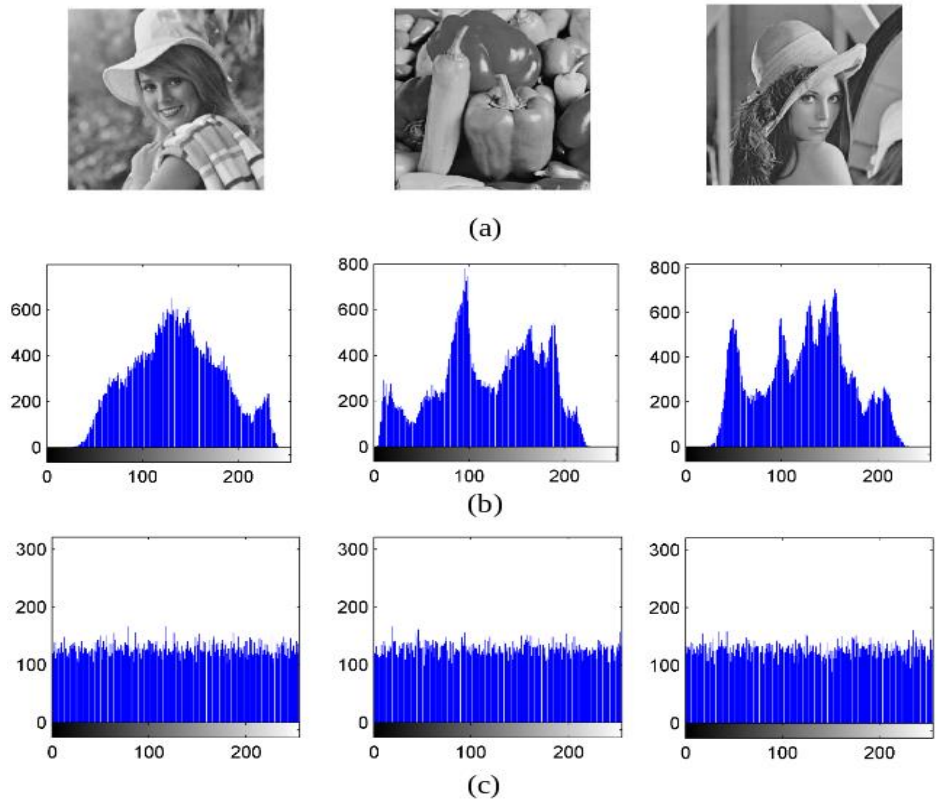

Figure 5: Histogram analysis (a) Plain Images, (b) Histogram of Plain Images, (c) Histogram of Ciphered image.

One method for figuring out how irregular the encoded picture is to use data entropy. For a grayscale picture to be viewed as irregular, the grayscale levels should be consistently disseminated. Closer to 8 is the data entropy that is expected for a code picture that seems to be clamor. One method for computing the worldwide data entropy is by using

$$H(Z) = -\sum_{i=0}^{255} Pr(GL_i)\, log_2 Pr(GL_i) \qquad (1.16)$$

where the probability of dark level *GLi's* event is addressed by *Pr* (*GLi*). In Table 2, you can see the data entropy of the encoded pictures. In comparison to Zhou et al. furthermore, comparable to Hu et al., the code's worldwide entropy is unrivaled. Furthermore, the overall entropy is moving toward its ideal worth.

Table 2: Global Entropy Analysis.

Test Images	**Global Entropy**			
	Plain Image	**Hu *et al.* 2017a**	**Zhou *et al.* 2014**	**Proposed**
Airplane	**6.7294**	**7.9936**	**7.9877**	**7.9945**
Barbara	**7.5838**	**7.9953**	**7.9886**	**7.9937**

Bee	**6.6953**	**7.9941**	**7.9890**	**7.9939**
Bobcat	**5.8494**	**7.9945**	**7.9892**	**7.9941**
Butterfly	**7.3075**	**7.9948**	**7.9889**	**7.9942**
Fishing Boat	**7.1583**	**7.9944**	**7.9885**	**7.9948**
Goldhill	**7.4450**	**7.9951**	**7.9891**	**7.9942**
Jelly Beans	**5.7286**	**7.9942**	**7.9891**	**7.9940**
Peppers	**7.5770**	**7.9945**	**7.9889**	**7.9936**
Splash	**7.2372**	**7.9938**	**7.9880**	**7.9943**

There is a huge level of association between adjoining pixels in an image, which is shown by the connection coefficient. The recommended strategy encodes the first picture as an irregular, commotion like picture. Thus, the scrambled picture need to have a low degree of adjoining pixel connection. 2,000 arbitrarily chosen adjoining pixels in every one of the three aspects are utilized to compute the relationship coefficient. This is the equation for ascertaining the connection coefficient:

$$r_{xy} = \frac{cov(x,y)}{\sqrt{D(x)D(y)}} \tag{1.17}$$

Where $cov(x,y) = \frac{1}{p}\sum_{i=1}^{P}[x_1 - E(x)][y_i - E(y)], \quad D(x) = \frac{1}{p}\sum_{i=1}^{p}[x_i - E(x)]^2$

and

$$E(x) = \frac{1}{p}\sum_{i=1}^{p} x_i \tag{1.18}$$

You can see the decorrelation between the adjoining pixels in the encoded picture in Table 3, which records the connection coefficients of the scrambled picture. Hu et al. what's more, Zhou et al. both got relationship coefficients that are comparable to what the proposed procedure produces.

Table 3: Comparison of Correlation Coefficient.

Test Image	**Direction**	**Correlation Coefficient of Plain Image**	**Correlation Coefficient of Ciphered Image**		
			Hu *et al.* 2017a	**Zhou *et al.* 2014**	**Proposed**
Airplane	**Horizontal**	**0.9394**	**0.0052**	**-0.0454**	**0.0044**
	Vertical	**0.9183**	**0.0068**	**0.0051**	**-0.0336**
	Diagonal	**0.8874**	**0.0062**	**-0.0330**	**0.0505**
Barbara	**Horizontal**	**0.9476**	**-0.0096**	**-0.0127**	**-0.0107**
	Vertical	**0.9662**	**-0.0218**	**0.0273**	**-0.0323**
	Diagonal	**0.9135**	**0.0050**	**-0.0023**	**0.0265**
Bee	**Horizontal**	**0.9847**	**0.0051**	**-0.0131**	**0.0065**

	Vertical	**0.9802**	**-0.0165**	**0.0034**	**0.0424**
	Diagonal	**0.9638**	**0.0403**	**-0.0127**	**0.0007**
Bobcat	**Horizontal**	**0.9761**	**-0.0309**	**0.0014**	**0.0117**
	Vertical	**0.9756**	**-0.0063**	**-0.0066**	**0.0330**
	Diagonal	**0.9602**	**-0.0134**	**-0.0059**	**-0.0214**
Butterfly	**Horizontal**	**0.9461**	**-0.0128**	**-0.0436**	**0.0347**
	Vertical	**0.9286**	**0.0162**	**0.0283**	**0.0361**
	Diagonal	**0.8965**	**0.0147**	**0.0274**	**-0.0079**

Figure 6 shows the relationship between's adjoining pixels in both the plain in addition to scrambled picture. As seen, there is major areas of strength for a between adjoining pixels in the simple picture while utilizing test pictures as a cameraman. The decorrelated pixels of the encoded picture are displayed in the figure underneath.

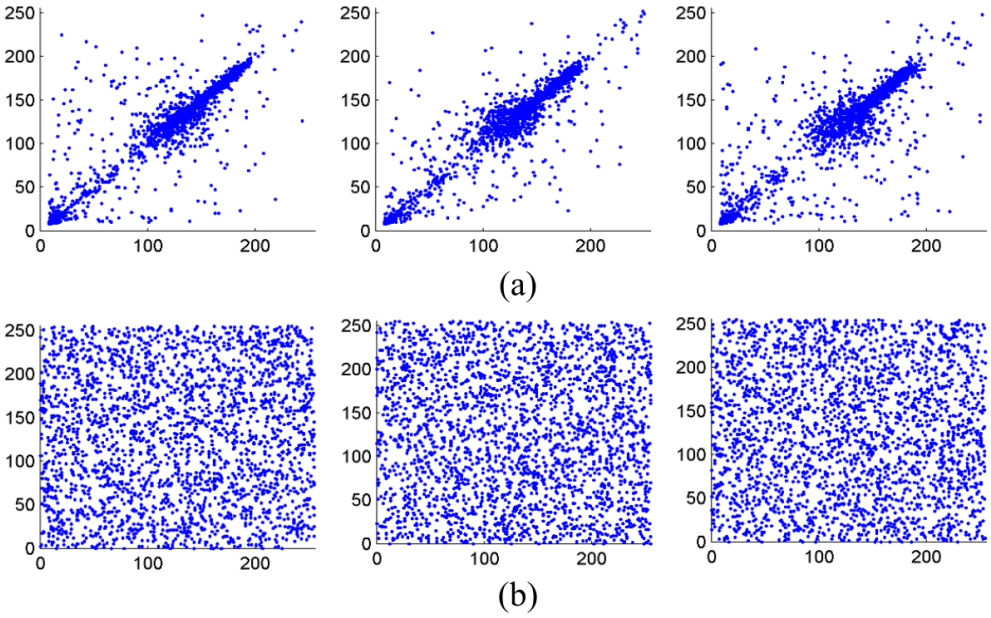

Figure 6: Scatter Plot of the Correlation Coefficient for the test image Cameraman (a) Plain Image (b) Ciphered Image.

V. SUMMARY

A scanty coding and compressive detecting-based encryption strategy is introduced in this paper. Utilizing a learnt word reference, we might recover the meager coding of the plain picture (Zhang, 2020). A blend of compressive sampling and irregular projection with a Gaussian estimation network considers the consolidated compression-encryption of pictures. The estimation is exposed to pseudorandom encryption and disarray-based piece scrambling to get the encoded picture. We outflanked Hu et al. furthermore, came near Zhou et al. concerning PSNR. (Zhao, 2020) The proposed approach beats Hu et al. furthermore, Zhou et al. regarding SSIM. The trial results exhibit that the recommended technique produces a cryptographically hearty code.

REFERENCES

[1] Chen, W., Xu, X., & Lin, C. (2018). A high-capacity and reversible image data hiding based on improved error correction coding and adaptive block partitioning. Multimedia Tools and Applications, 77(10), 13771-13793.

[2] Gong, L., Yang, Y., & Zhang, X. (2021). A novel two-stage image steganography with chaotic encryption and adaptive quantization. Signal Processing, 187, 107970.

[3] Li, B., Yang, Y., & Li, J. (2019). A robust and high-capacity image steganography based on multi-layer embedding and adaptive block partitioning. Multimedia Tools and Applications, 78(27), 37803-37832.

[4] Li, R., & Zheng, Y. (2020). A two-stage image steganography with enhanced security based on chaotic map and multiple-layer embedding. Journal of Systems and Software, 173, 110675.

[5] Li, Z., Zhang, L., & Liu, Y. (2021). A high-capacity and robust image steganography based on improved error correction coding and adaptive block selection. Multimedia Tools and Applications, 80(14), 10393-10413.

[6] Liu, Y., Yang, Y., & Zhu, X. (2021). Reversible image data hiding with multi-bitplane embedding based on histogram analysis and spatial local difference. Information Sciences, 550, 422-439.

[7] Luo, W., Qin, F., & Sun, W. (2019). A high-capacity and robust image steganography based on improved error correction coding and adaptive pixel selection. Signal Processing, 165, 226-238.

[8] Luo, W., Qin, F., & Sun, W. (2021). Enhanced image steganography based on chaotic encryption and multi-layer embedding of shared secret. Multimedia Tools and Applications, 80(23), 17049-17069.

[9] Qin, F., Sun, W., & Luo, W. (2019). A novel image steganography based on chaotic encryption and adaptive LSB substitution. Journal of Visual Communication and Image Representation, 71, 1-11.

[10] Wang, S., Wu, Y., & Sun, W. (2020). A robust and high-capacity image steganography based on dual-layer embedding and adaptive pixel adjustment. Multimedia Tools and Applications, 79(11), 7903-7924.

[11] Wu, X., Zheng, G., & Wang, X. (2020). A novel image steganography based on edge and texture adaptive embedding. IEEE Transactions on Circuits and Systems II: Express Briefs, 67(12), 2662-2666.

[12] Xu, W., Wang, B., & Wang, R. (2021). A robust and high-capacity image steganography based on dual-channel encryption and adaptive LSB modification. Journal of Visual Communication and Image Representation, 75, 102989.

[13] Xu, X., Li, W., & Lu, X. (2022). Two-stage image steganography based on hybrid local variance and frequency domain embedding. Multimedia Tools and Applications, 83(16), 19803-19827.

[14] Zhang, Y., Liu, Y., & Sun, X. (2020). A high-fidelity and high-capacity two-stage image steganography with reversible data embedding. IEEE Transactions on Information Forensics and Security, 15(12), 3954-3967.

[15] Zhao, L., Wu, Y., & Sun, W. (2020). A secure and high-capacity image steganography based on improved chaotic encryption and adaptive pixel adjustment. Multimedia Tools and Applications, 79(24), 18967-18990.